Mesonic spectral functions and transport properties in the quenched QCD continuum

A. Francis[(a)], O. Kaczmarek[(b)], M. Mueller[(b)], and F. Meyer[(b)]

[(a)] University of Mainz - Germany, [(b)] University of Bielefeld - Germany

We present new results on the reconstruction of mesonic spectral functions for three temperatures above T_c in quenched QCD. Making use of non perturbatively improved clover Wilson valence quarks allows for a clean extrapolation of correlator data to the continuum. For the case of vanishing momentum the spectral function is obtained by fitting the data to a well motivated ansatz. In the vector channel for light quarks the electrical conductivity of the hot medium, related to the origin of the spectral function at zero momentum, is computed from the resulting parameters at all three temperatures.

I. Motivation

The ongoing heavy ion collision experiments at different facilities all over the world necessitates a deeper theoretical understanding of the out of equilibrium phenomena encountered. The use of hydrodynamics to describe the collision process calls for accurately determined transport coefficients such as diffusion constants and viscosities [1].

From a theoretical point of view electromagnetic observables such as dileptons and photons constitute good probes of all stages of a collision within the "fireball" paradigm, as they only interact electromagnetically with the sorrounding plasma. They stem from decaying vector mesons as the latter ones are the currents in electromagnetic interactions among hadrons, described by the Vector Meson Dominance Model [2]. On the other hand, PHENIX and STAR experiments see enhancements in the measured dilepton rates in the low energy region of heavy ion collisions compared to proton-proton collisions [3] Since this regime is slightly above the deconfinement temperature, and thus one expects it to be strongly interacting, perturbative calculations are both conceptually difficult and show poor convergence for most observables. Utilizing numerical lattice QCD techniques on the other hand provides an inherently nonperturbative way to obtain needed correlation functions, though still being computationally expensive in the physical case and adding the necessity of an analytic continuation [4,5], resulting in its very own problems of obtaining above mentioned observable quantities.

Nevertheless a nonperturbative approach is indispensable in the energy regime slightly above T_c and thus ought to be addressed in this work.

II. The spectral function

Our goal is to compute lattice data of the **vector channel correlator**, because dilepton and photon rate are directly linked to (parts of) the vector correlator spectral function (SPF) as follows,

$$\frac{\mathrm{d}W}{\mathrm{d}\omega \mathrm{d}^3p} \sim \frac{\rho_V(\omega,\vec{p},T)}{(\omega^2-\vec{p}^2)(e^{\omega/T}-1)}\,, \qquad \omega\frac{\mathrm{d}R_\gamma}{\mathrm{d}^3p} \sim \frac{\rho_V^T(\omega=|\vec{p}|,T)}{e^{\omega/T}-1}\,.$$

This not only yields a direct connection of experimentally accessible and theoretically interesting quantities, but furthermore transport coefficients are generally related to SPFs via so called **Kubo formulae**. In case of the light vector particle SPF this leads to a simple formula for the electromagnetic conductivity,

$$\frac{\sigma}{T} = \frac{C_{em}}{6}\lim_{\omega\to 0}\frac{\rho_{ii}}{\omega}\,, \tag{1}$$

where different components of the vector SPF $\rho_H,\ H=V,ii,00$ are denoted by

- $\rho_V \equiv \rho_{ii}-\rho_{00}$ full vector SPF
- ρ_{ii} spatial vector SPF
- ρ_{00} temporal vector SPF

The (renormalized) Euclidean vector correlation functions are constructed as

$$J_H = Z_V\psi(x)\gamma_H\psi(x)$$
$$G_H(\tau,\vec{x}) = \langle J_H(\tau,\vec{x})J_H^\dagger(0,\vec{0})\rangle,$$

and projected to momenta $\vec{p}$:

$$G_H(\tau,\vec{p}) = \sum_{\vec{x}} G_H(\tau,\vec{x})e^{i\vec{p}\vec{x}}$$

The connection of the Euclidean correlator and the SPF, thus establishing the needed analytic continuation, is then given by the integral transformation

$$G_H(\tau,\vec{p}) = \int_0^\infty \frac{\mathrm{d}\omega}{2\pi}\rho_H(\omega,\vec{p},T)K(\omega,\tau,T) \tag{2}$$

$$K(\omega,\tau,T) = \frac{\cosh(\omega(\tau-\frac{1}{2T}))}{\sinh(\frac{\omega}{2T})} \tag{3}$$

with $K(\omega,\tau,T)$ being the integration kernel at finite temperature. The conceptual difficulties now lie in the inversion of eqn. (2), which is on the analytical level still a matter of mathematical discussion [5] and from the numerical standpoint an "ill posed problem": while having $N_\tau \sim \mathcal{O}(10)$ in typical finite T lattice simulations on the l.h.s, the desired resolution of the SPF as a function of ω on the r.h.s. of eqn. (2) is far larger, i.e. around $\mathcal{O}(1000)$.

III. A solution

There are two main ideas that try to soften this very fundamental problem by supplying additional information to the raw data.

1. The **Maximum Entropy Method (MEM)** is based on maximizing an entropy term while supplying a priori known, testable information (correlator data points) and a so called default model. The result is *the most probable* SPF given the former constraints.
2. By **specifiying an ansatz for the SPF and fitting** it to the correlator data points one is provided with an analytically known SPF parameterized by a few parameters. The ansatz should be phenomenologically well motivated and yet simple enough to allow for successful χ^2 minimization.

As opposed to MEM, which is inherently statistical, the latter method yields solid estimations of the SPF with systematical uncertainties stemming directly from the choice of the ansatz itself.

Looking for a suitable ansatz a good starting point is the free, non interacting case, corresponding to very high temperature, for which the vector SPF components ρ_H are analytically known:

$$\rho_{ii}^{\mathrm{free}}(\omega,T) = 2\pi T^2\omega\delta(\omega) + \frac{3}{2\pi}\omega^2\tanh(\frac{\omega}{4T}) \equiv \rho_{ii,<}^{\mathrm{free}} + \rho_{ii,>}^{\mathrm{free}}$$
$$\rho_{00}^{\mathrm{free}}(\omega,T) = 2\pi T^2\omega\delta(\omega).$$

Upon the influence of interactions the temporal component is not altered because the temporal part of the vector current J_0 is linked to the conserved net quark number and thus is independent of euclidean time. The quark number susceptibility $\chi_q = -\frac{1}{T}\int \mathrm{d}^3x\langle J_0J_0^\dagger\rangle = -\frac{1}{T}G_{00}$ is thus a constant, and the delta function in ρ_{00} remains there:

$$\rho_{00}^{\mathrm{free}} \to 2\pi\chi_q\omega\delta(\omega).$$

On the other hand, the spatial component does not feature such protection by symmetry and thus is modified. The naive and general expectation is that the delta peak melts and becomes broader and more analytic. To get an idea of its possible analytical structure, introducing and solving Langevin diffusion and Boltzmann gas toy models for heavy and light quarks, respectively, yields that the delta peak of the free case smears out into the shape of a Breit-Wigner peak [6].
Hence we choose our ansatz for the spatial part of the vector SPF to be composed of a Breit-Wigner peak for small frequencies ω and a slightly modified large ω part from the free vector SPF:

$$\rho_{ii}(\omega,T) = \chi_q c_{BW}\frac{\omega\Gamma}{\omega^2+(\Gamma/2)^2} + \frac{2}{3\pi}(1+k)\omega^2\tanh\left(\frac{\omega}{4\pi}\right) \tag{4}$$

with Γ, c_{BW}, κ parameterizing the resulting SPF. Note that for the modification of the large ω part $\kappa = \frac{\alpha_s}{\pi}$ holds at leading order.

III. Lattice data and continuum extrapolation

Lattice calculations have been done using a **nonperturbatively improved Wilson-Clover action** with **no dynamical sea quarks**. Runs were performed at three different temperatures $T = 1.1T_c, 1.2T_c, 1.45T_c$ with 3-4 increasingly finer lattices each. All valence quark masses are chosen to be small around $m_{\overline{MS}}(\mu = 2GeV) \sim \mathcal{O}(10MeV)$. Note that for the two lowest temperatures the aspect ratio is fixed to $N_s/N_t = 3$, ensuring a constant physical volume, while for the $T = 1.45T_c$ lattice finite volume effects were verified to be small.

N_σ	N_τ	β	κ	1/a[GeV]	#
$T = 1.1T_c$					
32	96	7.192	0.13440	9.65	314
48	144	7.544	0.13383	13.21	358
64	192	7.793	0.13345	19.30	242
$T = 1.2T_c$					
28	96	7.192	0.13440	9.65	232
42	144	7.544	0.13383	13.21	417
56	192	7.793	0.13345	19.30	273
$T = 1.45T_c$					
16	128	6.827	0.13495	6.43	191
24	128	7.192	0.13440	9.65	340
32	128	7.457	0.13390	12.86	255
48	128	7.793	0.13340	19.30	456

Using these lattices, ratios of correlation functions

$$R_{ii} = \frac{T^2}{\chi_q}\frac{G_{ii}(\tau T)}{G_V^{free,lat}(\tau T)}, \qquad \chi_q = -G_{00}/T \tag{5}$$

are formed for each lattice per temperature available. The spatial correlation function is normalized by the quark number susceptibility χ_q to cancel the necessary renormalization and furthermore normalized by the free full vector correlation function to cancel the exponential fall-off.

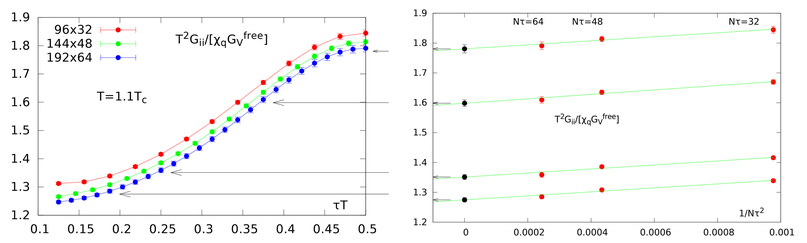

Figure 1: *Left:* The computed ratios as a function of $\tau T = \tau_{lat}/N_t$. *Right:* The actual linear extrapolation procedure in a^2 for four selected values of τT with the extrapolation results colored in black.

These ratios are extrapolated to the continuum via a linear fit in the squared lattice constant a^2 due to the improved action. Note that the resulting continuum ratio is computed for all N_t^{max} data points of the largest lattice per temperature by spline interpolating the ratios on the smaller lattices. The whole resulting continuum correlator for this temperature is shown in fig. (2).

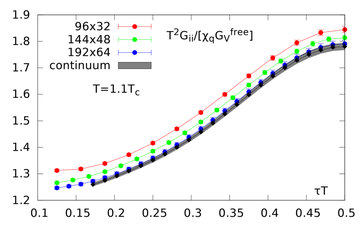

Figure 2: The resulting extrapolation of ratio eqn. (5)

Aside from the ratio of correlation functions also the continuum value of the quark number susceptibility χ_q is determined in the same fashion after obtaining $\chi_q^{N_t}$ from the constant correlator G_{00} at finite lattice spacing. However, these now have to be renormalized using the proper nonperturbatively determined renormalization constants [7]. The continuum result for χ_q is needed in the computation of the electrical conductivity shown in the next section.

IV. Obtaining the SPF

In order to obtain estimators for the parameters of the fit ansatz eqn. (4) the **continuum extrapolated correlators are used as input data for the fitting process**. Having determined the parameters the electrical conductivity of the QGP is immediately available from the Kubo formula eqn. (1) as

$$\frac{\sigma}{T} = \frac{2}{3}C_{em}\chi_q\frac{c_{BW}}{\Gamma},$$

where $C_{em} = \sum_i Q_i^2$ and Q_i being the charges of the involved quark flavors. Note that, as it is proportional to the origin of the SPF, it does not depend on the parameter κ governing the large ω behavior. Expanding the integration kernel eqn. (3) for small frequencies yields

$$K(\omega,\tau,T) = \frac{2T}{\omega} + \left(\frac{1}{6T} - \tau + T\tau^2\right)\omega + \mathcal{O}(\omega^3),$$

showing that the contribution of the low frequency part to the correlation function is nearly a constant given $\tau T \in [0, 0.5]$. Hence the information about the peak region of the spectral function lies in the weakly τ dependent region of the correlator, i.e. around the midpoint, see [8] for further discussion. In order to improve the signal coming from this region, any additional information to the correlator data is usefull. One possibility, chosen in this work, is to define **thermal moments** $G_H^{(n)}$ as Taylor coefficients of the correlation function,

$$G_H(\tau T) = \sum_{n=0}^{\infty} G_H^{(n)}\left(\frac{1}{2}-\tau T\right)^n$$

$$G_H^{(n)} = \frac{1}{n!}\frac{d^nG_H(\tau T)}{d(\tau T)^n}\bigg|_{\tau T=1/2} = \frac{1}{n!}\int_0^\infty\frac{\mathrm{d}\omega}{2\pi}\left(\frac{\omega}{T}\right)^n\frac{\rho_H(\omega)}{\sinh(\omega/(2T))}$$

and to form the **midpoint subtracted correlator ratio**

$$\Delta_H(\tau T = 1/2) \equiv \frac{1}{\chi_q}\frac{G_H(\tau T)-G_H^{(0)}}{G_H^{free}(\tau T)-G_H^{(0),free}}\bigg|_{\tau T=1/2} = \frac{1}{\chi_q}\frac{G_H^{(2)}}{G_H^{(2),free}}\,. \tag{6}$$

The value of $\Delta_H(\tau T = 1/2)$ is then used as an additional data point for the fit as it essentially encodes information on the curvature of the correlation function ratio at the midpoint.

The fits are done by a Levenberg-Marquardt minimization algorithm and using a standard gaussian quadrature for the integral of eqn. (2).

As mentioned in section *III*, a very large part of the error on the results will be a systematic one, because an important part in overcoming the "ill-posed"-ness of the inversion problem is to provide the functional form of the SPF as additional information: the structure of our fit ansatz, or, more specifically, the choice of the Breit-Wigner peak as a "melted delta" peak. In order to check on an effect in changing the ansatz, a parameterized low ω cutoff is multiplied into the free part of the ansatz,

$$\theta(\omega_0,\Delta_\omega) = \left(1+\exp((\omega_0^2-\omega^2)/(\omega\Delta_\omega))\right)^{-1}, \tag{7}$$

This way the form of the ansatz can be changed in a controlled and continuous way, the Breit-Wigner peak reacting to cutting off the early onset of the large ω free part in the ansatz. Upon increasing ω_0 at a fixed but small $\Delta_\omega \sim 0.1$ the resulting electrical conductivity rises as the Breit-Wigner peak has to adapt to the decreasing influence the free part has on the low to intermediate ω regime. At some point the fit quality becomes much worse and the peak cannot account anymore for the missing contribution of the free part. Thus we choose the upper error bound. The procedure is illustrated in fig. (3).

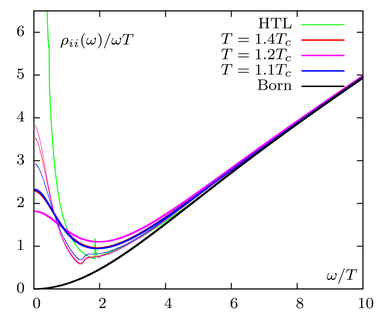

Figure 3: The low ω cutoff varied to yield final tolerable fit qualities, drawn for all three temperatures. The thin lines are the error estimations.

V. Results

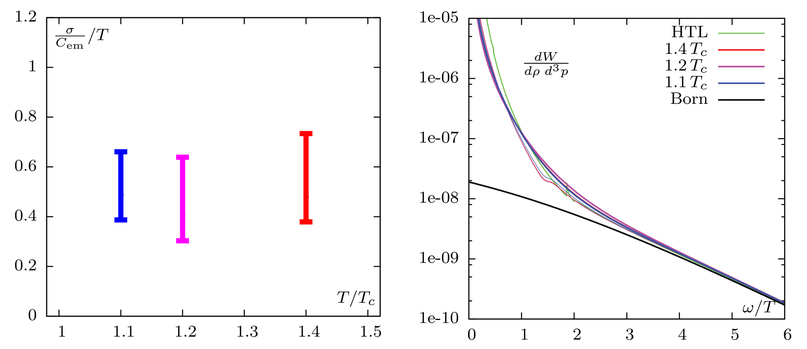

Figure 4: *Left:* The results for the electrical conductivity. The error stems from the systematic error analysis procedure described above. *Right:* The result for the low energy dilepton production. Note the agreement with the HTL result in green for intermedate and large frequencies.

The results for the electrical conductivity and the dilepton rate are shown in fig. (4), note that the factor C_{em} is divided out in the conductivity plot. At the current size of the errorbars it is not possible to make a statement about the temperature dependence of the conductivity, though a rise with temperature is expected.

The dileptonrate is evaluated at zero momentum $\vec{p}$, as all correlators in this work were projected to zero momentum. Note the free case labeled "Born" coinciding for large frequencies and the HTL result qualitatively agreeing with our nonperturbative result at intermediate and large frequencies. The former reflects that the parameter in the ansatz governing the large ω behaviour turns out to be very small ($\sim \mathcal{O}(10^{-2})$ for all three temperatures, thus the high frequency part of the ansatz is confirmed to be a good choice.

Similar nonperturbative studies for comparison can be found in e.g. [9,10].

VI. Conclusion / Outlook

For each of three different temperatures above T_c quenched lattices with decreasing lattice spacings have been produced. Using Wilson-Clover valence fermions correlation function data has been extrapolated to the continuum using a linear ansatz in a^2. Using a well motivated fit ansatz the spatial component of the vector spectral function has been constructed and thus the electrical conductivity of the plasma and the dilepton production rate obtained. An idea to assess the systematic error on the result has been implemented. For a more detailed background also see [11,12].

As future plans

- the reassessment of the systematical error and a possible study of the temperature dependence of the transport properties are attempted.
- The analysis of spectral functions at finite momentum building up on the methods used so far is on the way.
- The inclusion of dynamical sea quarks now becomes possible utilizing increasing computational power available.

VII. References

[1] U. Heinz, R. Snellings, Ann. Rev. Nucl. Part. Sci. **63** (2013) 123.
[2] D. Schildknecht, Acta Phys. Polon. B **37** (2006) 595.
[3] PHENIX PRC81, 034911 (2010).
[4] F. Karsch, H. W. Wyld, Phys. Rev. D 35, 2518 (1987).
[5] H. B. Meyer, Eur. Phys. J. A **47** (2011) 86.
[6] J. Hong, D. Teaney, Phys.Rev.C82 (2010) 044908.
[7] M. Lüscher, S. Sint, R. Sommer, H. Wittig, Nucl. Phys. B491, (1997) 344.
[8] G. Aarts and J. M. Martinez Resco, Nucl. Phys. Proc. Suppl. **119** (2003) 505.
[9] A. Amato, G. Aarts, C. Allton, P. Giudice, S. Hands and J. I. Skullerud, Phys. Rev. Lett. **111** (2013) 172001.
[10] B. B. Brandt, A. Francis, H. B. Meyer and H. Wittig, JHEP **1303** (2013) 100.
[11] H. T. Ding et. al., Phys.Rev. D83 (2011) 034504 [12] O. Kaczmarek, M. Müller, arXiv:1312.5609